Advanced Journal of Chemistry-Section A

Journal homepage: www.ajchem-a.com

Original Research Article

A Thermodynamic Investigation of the Interaction of Ferric (Fe^{3+}) Ion with (100, 110) Pyrite and (001) Chalcopyrite Surfaces Using the Density Functional Theory Study

Valeh Aghazadeh [1], Bahram Rezai [2], Hossein Nourmohamadi [2] *

[1] *Mineral Processing, Department of Mining Engineering, Sahand University of Technology, Tabriz, Iran*
[2] *Mineral Processing, Department of Mining Engineering, AmirKabir University of Technology, Tehran, Iran*

ARTICLE INFO

Article history

Submitted: 10 June 2023
Revised: 03 July 2023
Accepted: 06 July 2023
Available online: 08 July 2023
Manuscript ID: AJCA-2306-1378
Checked for Plagiarism: Yes

DOI: **10.22034/AJCA.2023.397689.1378**

KEYWORDS

Thermodynamic
Sulfide
Pyrite
Chalcopyrite
Ferric ion
Density functional theory

ABSTRACT

As a heterogeneous catalyst, Pyrite increases chalcopyrite oxidation by creating more cathodic points and enhancing electron transfer to ferric (Fe^{3+}) ions. In this study, the interaction of ferric ions with 100, 110 pyrite surfaces and 001-S, M (M= Cu and Fe) chalcopyrite surfaces was investigated using the Density functional theory (DFT) method and Material Studio software. The results showed that Fe^{3+} ion reacted well with the desired surfaces, and free energies were negative in the 25-275 °C temperature range, and interaction enthalpy increased linearly with increasing temperature. However, the two surfaces of 110 pyrite and 001-S chalcopyrite were more active than other surfaces, and a stronger reaction occurred between the ferric ion and that surfaces. Also, due to the strong metal-sulfur bond, the free energy of ferric ion interaction with the 001-M surface of chalcopyrite increased by increasing temperature. However, on the other surfaces, free energy was reduced in the presence of sulfur atoms.

GRAPHICAL ABSTRACT

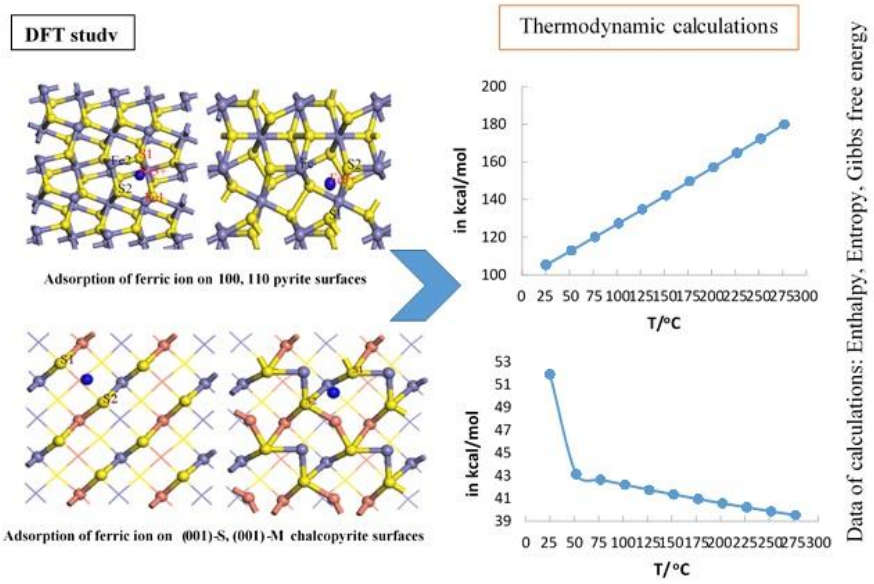

* Corresponding author: Nourmohamadi, Hossein
✉ E-mail: ghnpme@gmail.com, h.nourmohamadi@aut.ac.ir

Introduction

Chalcopyrite($CuFeS_2$) is the world's most important copper source [1-3]. The ferric sulfate is the most common oxidation agent due to the simplicity of the process and low cost [4,5]. The chalcopyrite leaching is initially fast but is disrupted due to forming a passive layer [6]. Most of the chemical or electrochemical research has focused on oxidative processes or redox, especially ferric (Fe^{3+}) ions. Some rely on the important role of the potential on the chalcopyrite leaching, in which increasing of Fe^{3+} ion is increased solution potential [6-11]. The reduction of Fe^{3+} ion is linearly related to temperature, and its reduction is increased with increasing temperature. The activation energy in the 25 °C is 76.8-87.7 kJ/mol, while the activation energy for electron transfer through elemental sulfur is 80-96 kJ/mol, reported in the literature [7-13]. Various oxidants such as carbon, oxygen, hydrogen peroxide, pyrite (FeS_2), and metal ions (Ag^{1+}, Hg^{1+}) have been investigated to improve the leaching of chalcopyrite [14-17]. In the meantime, pyrite as an accompanying mineral and availability are among the things that have attracted the attention of researchers. Pyrite leads to the increase of cathode points on the surface, which improves the dissolution of chalcopyrite with the help of the galvanic effect and acts as a heterogeneous catalyst [15,18]. Galvanic interaction between sulfides results in electron transfer from less rest potential minerals to more rest potential minerals. Sulfide mineral with larger rest potential is more stable in the medium, and as a conductor, it transfers electrons from the adjacent sulfide surface (less potential and unstable) [19]. Miller and Chahremaninejad *et al*. believe that the electrochemical reaction of chalcopyrite leaching depends on the charge transfer between the particle surface and the Fe^{3+} ion [20,21].

In the presence of pyrite, ions increased in the solution-solid interface, thereby reducing the resistance to electron transfer [22,23]. Yubiao Li *et al*. suggested that pyrite causes the oxidation of chalcopyrite in the presence of Fe^{3+} ions by preventing the formation of hydrogen sulfide on the surface and increasing the solubility potential [24]. The Fe^{3+} ion interacts well on clean surfaces of pyrite and chalcopyrite, but its reduction is more rate on the pyrite surface. Also, the rate of reduction on galvanic coupling, pyrite/chalcopyrite, is greater than that of solitary chalcopyrite, and the corresponding current density is higher in the presence of pyrite [22,25].

Some studies have been conducted to evaluate the structure, surfaces, and electrical resistance of chalcopyrite and pyrite [26-30]. Studies by Hang *et al*. on the 100 and 110 pyrite surfaces revealed that the 100 surface is more stable, and the electrostatic properties of the surfaces depend on the iron and sulfur atoms on the surface [26]. Also, the adsorption of oxygen molecules on the 001 surface of chalcopyrite occurs near iron atoms (due to the lower energy barrier of iron atoms) and oxygen showed less tendency to react with other surface atoms [27-29]. The formation of disulfide and the reduction of iron (III) ions to iron (II) on the surface are the most probable events that can occur due to the reconstruction of chalcopyrite surfaces, which is mentioned in the theoretical studies of Oliveira *et al*. [30].

In this paper, due to the importance of chalcopyrite leaching in the presence of Fe^{3+} ion, the interaction of Fe^{3+} ion with 001 surface of chalcopyrite and 100, 110 surfaces of pyrite by using density functional theory (DFT) and material studio software were investigated. The 001 surface of chalcopyrite and the 100, 110 pyrite surfaces are pyrites and chalcopyrite main cleavages. This study was conducted to better identify the behavior of pyrite and chalcopyrite in the presence of Fe^{3+} ions because the oxidation

of chalcopyrite slows down over time, and the amount of copper extraction decreases.

Computational details

Previous studies have indicated that the DFT is among the most versatile and popular methods to investigate electronic structure of solids [31-33]. Bulk pyrite, chalcopyrite, and all surface relaxation calculations were optimized with the Perdew–Burke–Ernzerhof (PBE) density functional as implemented in the Dmol^3 code [34]. Chalcopyrite bulk and pyrite space groups are I-42d and Pa3, respectively. Cell parameters of chalcopyrite are: a = b = 5.289 Å, c = 10.4230 Å. The pyrite unit cell is cubic, and each Fe atom is coordinated with six atoms of S, and each S atom is coordinated with three atoms of Fe and one S atom [35,36].

Optimization of bulk pyrite and chalcopyrite were performed with 4×4×4 and 3×3×1 K-points, respectively. A double numerical (DND) basis set and semi-core pseudopotential (DSPPs) were employed in the DFT calculations. Calculations on the relaxed surfaces and adsorption study were performed on 2×2 supercell surface for 100 and 2×1 for 110 surfaces of pyrite by using the COSMO method (water solvent) [37]. The number of layers for the 110 and 100 surfaces are 6 and 7 layers, according to **Figure 1**.

Furthermore, calculations of chalcopyrite surfaces were performed on supercell surface 2×2, with 2×2×1 k-points, using the COSMO method (water solvent), as demonstrated in **Figure 2**. The number of layers for the 001-S and the 001-M surfaces is 5 and 6 layers, respectively. Vacuum region equal to 20 Å was applied to prevent the interaction between layers, and the bottom layers were fixed during the geometry optimizations.

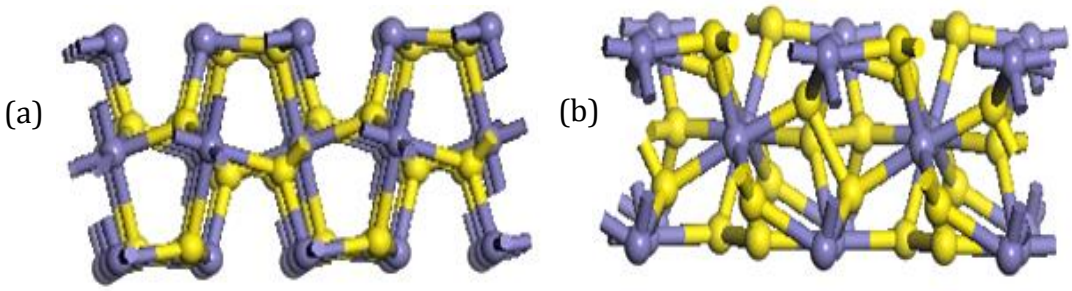

Figure 1. The 100 and 110 surfaces of pyrite: (a) 100 surface, (b) 110 surface

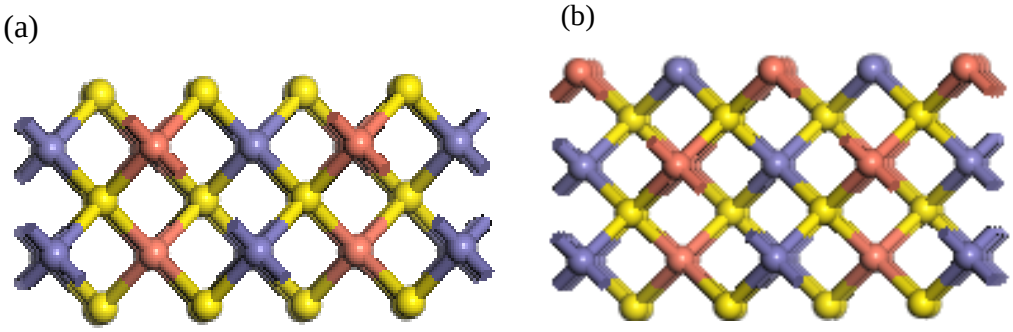

Figure 2. The 001-S and M surfaces of chalcopyrite: (a) 001-S surface, (b) 001-M surface

After preparing the surfaces, the interaction of Fe^{3+} ion with surfaces of chalcopyrite and pyrite was investigated. According to earlier studies, the Fe^{3+} ion tends to be adsorbed over the surfaces where sulfur atoms are present. **Figures 3** and **4** reveal the most stable configurations of Fe^{3+} ion adsorbed on the surfaces [38,39].

The thermodynamic calculations were performed under the computational conditions mentioned. Thermodynamic studies include changes in enthalpy, entropy, and free energy in the temperature range between 25 - 275 °C.

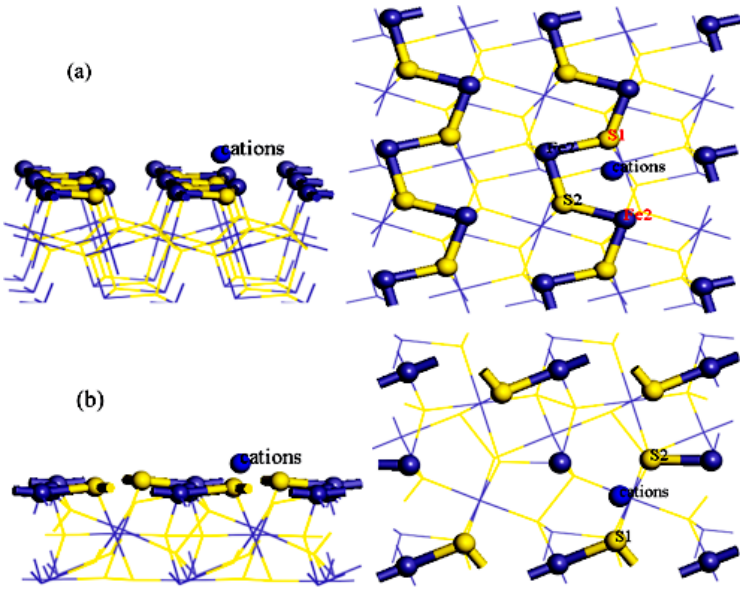

Figure 3. Fe^{3+} position on the surface of pyrite: (a) 100 surface, (b) 110 surface

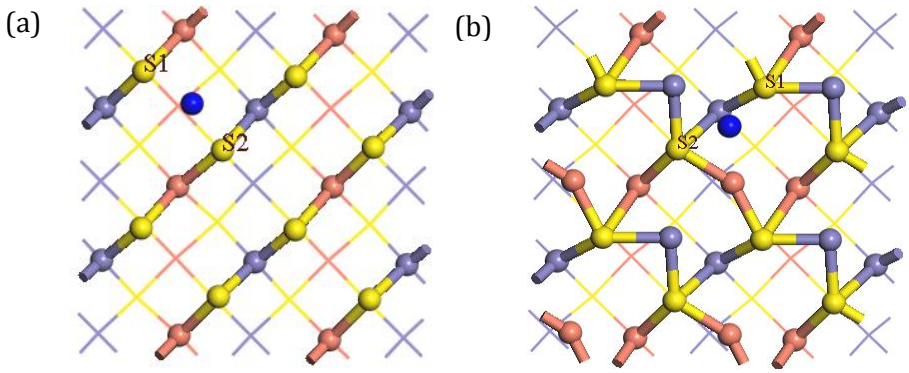

Figure 4. Fe^{3+} position on the surface of chalcopyrite: (a) 001-S surface, (b) 001-M surface

Results and discussion

Enthalpy

To better understand the interaction of Fe^{3+} ions with the surfaces, the thermodynamic parameters for reducing Fe^{3+} were also obtained at 25-275 °C and 1 atm. The interaction of the Fe^{3+} ion with 100 and 110 pyrite surfaces is an electrostatic reaction that leads to electron transfer to the Fe^{3+} ion [40]. According to previous studies, the dissolution of chalcopyrite

in an acidic environment in the presence of pyrite increases by increasing temperature and is temperature dependent [5,12]. As shown in **Figure 5**, the enthalpy value is positive and increases at both surfaces with increasing temperature.

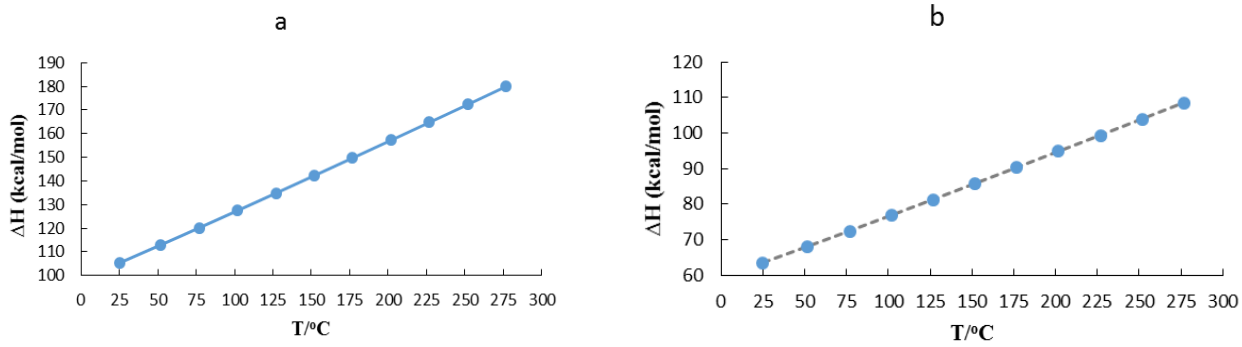

Figure 4. Enthalpy of Fe^{3+} ion interaction with pyrite surfaces: (a) 100 surfaces, (b) 110 surface

The trend of changes for 001-S and 001-M chalcopyrite surfaces was similar to pyrite, which positively and linearly increased**.** However, energy values for the 001-M surface were further and extended the range. The enthalpy changes of the Fe^{3+} ion interaction on the chalcopyrite surfaces are shown in **Figure 6**.

In addition, the positive enthalpy values on the 110 pyrite surface and the 001-S chalcopyrite surface were lower than other surfaces, and 110 and 001-S surfaces had better conditions for reaction with ferric ion, which is consistent with previous data [26,39].

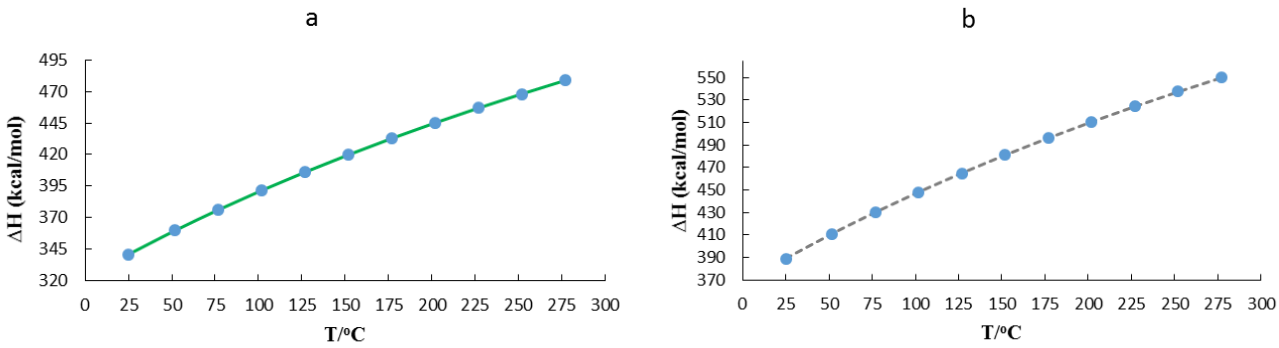

Figure 6. Enthalpy of Fe^{3+} ion interaction with chalcopyrite surfaces: (a) 001-S surface, (b) 001-M surface

Free energy

As Equation 1 shows, Fe^{3+} ion can be reduced to the Fe^{2+} ion over the surfaces**.**

$$Fe^{3+} + e^{-} \longrightarrow Fe^{2+} \quad (1)$$

As a result, equation 2 was used to obtain the free energy changes of this reaction:

$$\Delta G = G_{Fe2+} - (G_{Fe3+} + G_e) \quad (2)$$

Where G_{Fe2+} and G_{Fe3+} are the free energy of the adsorbed Fe^{2+} and Fe^{3+} ions, respectively, and G_e is the Gibbs free energy of an electron. When the Fe^{3+} ion reacted with the surface, it received electrons from the surface and converted to the Fe^{2+} ion. The surface charge difference before

and after Fe^{3+} ion adsorption equals the amount of electron charge. The free energy values for the surfaces were obtained as negative at different temperatures multiplied by -1 for better representation, as shown in **Figures 7** and **8**. According to Figure 7, the free energy of Fe^{3+} ion interaction on the pyrite surfaces decreased by increasing temperature. This decrease was more slope for the 110 pyrite surfaces, in Figure 7a, and less for the pyrite 100 surfaces, in Figure 7, b. However, by comparing the amounts of free energy at different temperatures, we can find that 110 surface has a stronger interaction with Fe^{3+} ion, and its free energy is much higher than 100 surfaces.

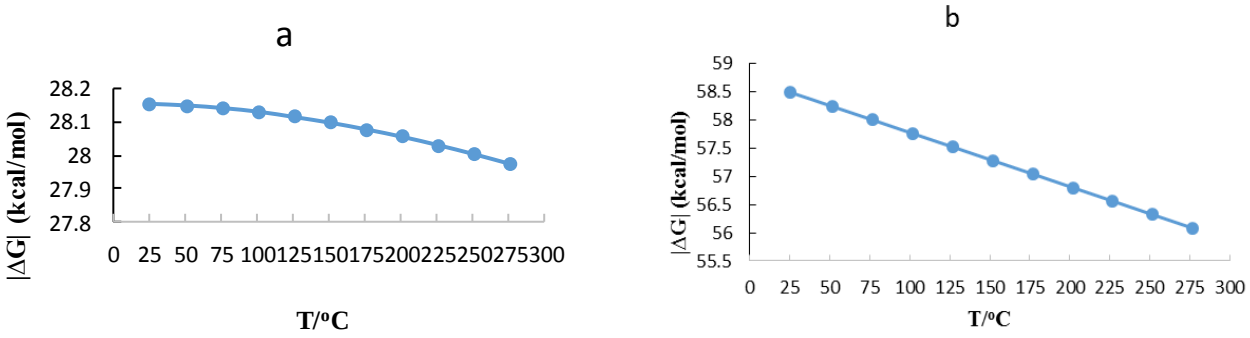

Figure 7. Free energy of Fe^{3+} ion interaction with pyrite surfaces: (a) 100 surface, (b) 110 surface

The reaction of Fe^{3+} ion with chalcopyrite surfaces was well performed, and the negative free energy values at the desired temperatures confirm it. According to Figure 8a, the free energy decreased with increasing temperature for the 001-S surface. The maximum value was obtained at 25 °C and decreased with a slight slope at different temperatures.

According to Figure 8b, for the 001-M surface increasing the temperature caused an increase in the free energy, however the range of energy changes for the 001-M surface was lower than for the 001-S surface that at the ambient temperature (25 °C) the interaction of Fe^{3+} ion over the 001-S surface

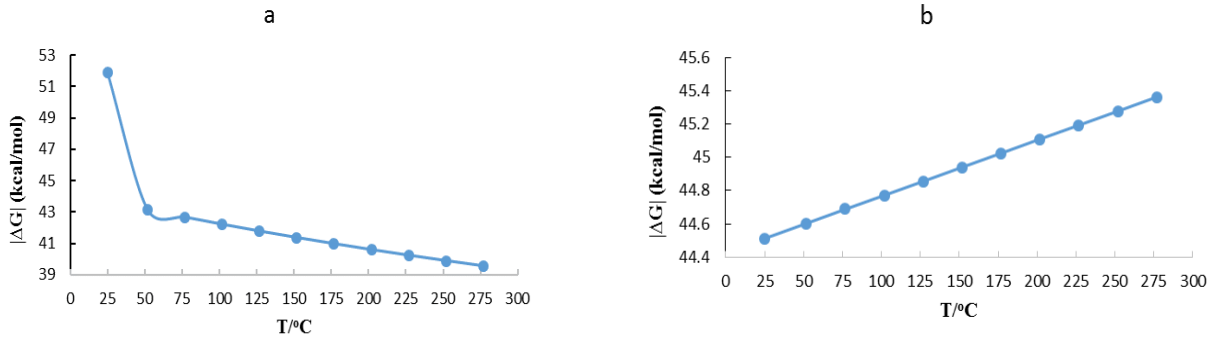

Figure 8. Free energy of Fe^{3+} ion interaction with chalcopyrite surfaces: (a) 001-S surface, (b) 001-M surface

Entropy

To investigate the effect of entropy on the interaction of Fe^{3+} ions with surfaces in the desired temperature range of 25-275 °C, equation 3 was used. At both the 100 and 110 surfaces, the curve show the positive effect of the entropy curve's trend shows the entropy's positive effect on the lese temperature.

$$\Delta G = \Delta H - T\Delta S \quad (3)$$

Where ΔG, ΔH, ΔS, and T are the free energy, enthalpy, entropy, and temperature, respectively. According to **Figure 9**, the entropy of the Fe^{3+} ion interaction decreased with the 100 and 110 pyrite surfaces. However, the entropy values for 100 surfaces, in Figure 9, a, were more significant.

Similar to the pyrite, entropy decreased for the 001-S and 001-M surfaces by increasing the temperature and was associated with a downtrend, as the **Figure 10** The more considerable entropy value at different temperatures for the 001-M surface than the 001-S surface can result from the more significant irregularity of the surface and the presence of metal atoms and reduced coordination [40,41]. The presence of sulfur atoms and the decrease in the coordination of metal atoms is caused by the 001-M surface activated electrostatically [41]. Overall, an increase in the temperature has decreased the entropy for both surfaces. However, its positive effect on the interaction of Fe^{3+} ions on the chalcopyrite surfaces was significant.

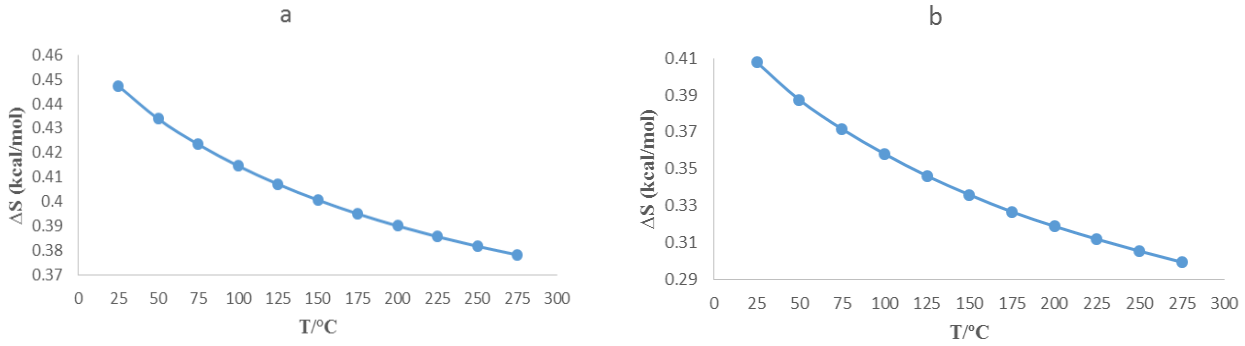

Figure 9. Entropy of Fe^{3+} ion interaction with pyrite surfaces: (a) 100 surface, (b) 110 surface

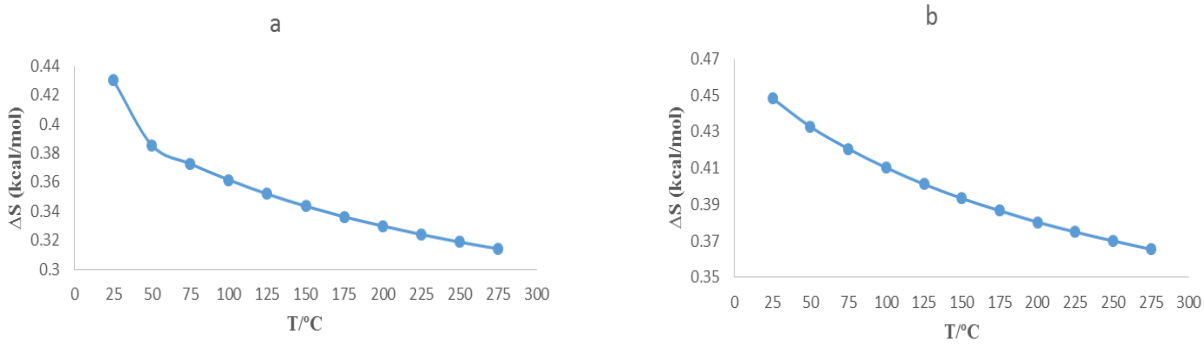

Figure 10. Entropy of Fe^{3+} ion interaction with chalcopyrite surfaces: (a) 001-S surface, (b) 001-M surface

According to the results obtained, the interaction of Fe^{3+} ion with pyrite and chalcopyrite surfaces was well performed, but the free energy values were further for the 110 surfaces of pyrite and 001-S surface of chalcopyrite [38,42]. More significant free energy and the enthalpy in the different temperatures for 110 surfaces indicated stronger interactions of Fe^{3+} ions with this surface. At 25 °C, free energy values for both surfaces of 110 and 001-S were more than 50 kcal/mole. The decrease in free energy at the 001-S surface may be related to more sulfur atoms, because sulfur-sulfur bonds are weaker than metal-sulfur bonds [29].

Conclusion

In the present study, the interaction of Fe^{3+} ion with the surfaces (100,110) of pyrite and (001-S, 001-M) chalcopyrite surfaces has been investigated by thermodynamic aspect. The Fe^{3+} ion has interacted with the surfaces of pyrite and chalcopyrite, and the electron exchange between the surfaces and the active species (Fe^{3+}) occurred well. Thermodynamic studies (enthalpy, entropy, free energy) showed the interaction of Fe^{3+} ion with surfaces as possible, and the active species tends to be absorbed on surfaces. In the 25-275 °C temperature range, the reaction enthalpy was linear and had an increasing (positive) trend. Also, negative interaction free energy was obtained in the desired temperature range, which can be a spontaneous reaction.

A comparison of thermodynamic data showed that two 110 pyrite and 001-S chalcopyrite surfaces are more active electrostatically. In addition, the decreasing trend of free energy for the 001-S surface was associated with a greater slope, which could be related to the presence of sulfur atoms on the surface. The structure of sulfur atoms can change under the influence of temperature, affecting the exchange of electrons between the surface and the Fe^{3+}ion. In general, the interaction of ferric ions with surfaces is an electrostatic reaction. The reaction depends on the favorable conditions for the transfer of electrons from valence band orbitals (Fe^{3+} ion) to the surface, which can change under the influence of temperature.

Acknowledgment

The authors acknowledge the support of Amirkabir and Sahand universities for carrying out this research.

Disclosure statement

The authors declare that they have no conflict of interest.

Orcid

Valeh Aghazadeh: 0000-0003-1833-6525
Bahram Rezai: 0000-0002-6050-3641
Hossein Nourmohamadi: 0000-0003-1463-0591

References

[1] E.M. Córdoba, J.A. Muñoz, M. Blázquez, F. González, A. Ballester, *Hydrometallurgy*, **2008**, *93*, 81–87. [CrossRef], [Google Scholar], [Publisher]

[2] S.M.S. Azghdi, K. Barani, *Min. Metall. Explor.*, **2018**, *35*, 141–147. [CrossRef], [Google Scholar], [Publisher]

[3] D. Yang, M. Kirke, F. Rong, C. Priest, *Anal. Chem.*, **2019**, *91*, 1557–1562. [CrossRef], [Google Scholar], [Publisher]

[4] J.B. Dutrizac, *Metall. Mater. Trans.*, **1981**, *12*, 371–378. [CrossRef], [Google Scholar], [Publisher]

[5] M.M. Antonijevic, G.D. Bogdanovic, *Hydrometallurgy*, **2004**, *73*, 245–256. [CrossRef], [Google Scholar], [Publisher]

[6] C. Klauber, A. Parker, V. Bronswijk, W. Watling, *Int. J. Miner. Process.*, **2001**, *62*, 65–69. [CrossRef], [Google Scholar], [Publisher]

[7] T. Hirato, H. Majima, Y. Awakura, *Metal. Trans. B*, **1987**, *18*, 489–496. [CrossRef], [Google Scholar], [Publisher]

[8] E. Córdoba, J. Muñoz, M. Blázquez, A. Ballester, *Hydrometallurgy*, **2008**, *93*, 88–96. [CrossRef], [Google Scholar], [Publisher]

[9] G. Warren, M. Wadsworth, S. El-raghy, *Metal. Trans. B*, **1982**, *13*, 571–579. [CrossRef], [Google Scholar], [Publisher]

[10] N. Hiroyoshi, S. Kuroiwa, H. Miki, M. Tsunekawa, T. Hirajima, *Hydrometallurgy*, **2004**, *74*, 103–116. [CrossRef], [Google Scholar], [Publisher]

[11] D. Nava, I. González, D. Leinen, J.R. Ramos-Barrado, *Electrochimica. Acta*., **2004**, *53*, 4889–4899. [CrossRef], [Google Scholar], [Publisher]

[12] K. Nyembwe, E. Fosso-Kankeu, F.B. Waanders, *Minerals*, **2021**, *11*, 963–972. [CrossRef], [Google Scholar], [Publisher]

[13] Y. Guikuan, *Speciation of the sulfuric acid-ferric sulfate-ferrous sulfate-water system and its application to chalcopyrite leaching kinetics up to 150 °C*, thesis, university of British Columbia, **2015**. [CrossRef], [Google Scholar], [Publisher]

[14] Dreisinger D, *Hydrometallurgy*, **2003**, *83*, 10–20. [CrossRef], [Google Scholar], [Publisher]

[15] D.G. Dixon, D.D. Mayne, K.G. Baxter, *Can. Metal. Quart.*, **2008**, *47*, 327–336. [CrossRef], [Google Scholar], [Publisher]

[16] N. Kawashima, J. Li, A.P. Chandra, *Adv. Colloid. Interface. Sci*., **2013**, *197*, 1–32. [CrossRef], [Google Scholar], [Publisher]

[17] H. Nakazawa, *Hydrometallurgy*, **2008**, *177*, 100–108. [CrossRef], [Google Scholar], [Publisher]

[18] G. Nazari, D.G. Dixon, D.B. Dreisinger, *Hydrometallurgy*, **2012**, *113*, 122-130. [CrossRef], [Google Scholar], [Publisher]

[19] R. Cruz, G.T. Lapidus, I. González, M. Monroy, *Hydrometallurgy*, **2005**, *78*, 198–208. [CrossRef], [Google Scholar], [Publisher]

[20] A. Ghahremaninezhad, D.G. Dixon, E. Asselin, *Hydrometallurgy*, **2012**, *125*, 42–49. [CrossRef], [Google Scholar], [Publisher]

[21] J.D. Miller, P.J. McDonough, H.Q. Portillo, *Min. Metall. Explor*, **1981**, *1*, 327–338. [Google Scholar]

[22] OG. Olvera, L. Quiroz, DG. Dixon, E. Asselin, *Electrochimica. Acta*, **2014**, *127*, 7–19. [CrossRef], [Google Scholar], [Publisher]

[23] Y. Li, G. Qian, J. Li, AR. Gerson, *Metals*, **2015**, *5*, 1566–1579. [CrossRef], [Google Scholar], [Publisher]

[24] M. Hong, X. Huang, X. Gan, G. Qiu, *Miner. Eng*., **2021**, *172*, 107145. [CrossRef], [Google Scholar], [Publisher]

[25] D. Majuste, V.S.T. Ciminelli, K. Osseo-Asare, M.S.S. Dantas, *Hydrometallurgy*, **2012**, *113*, 167–176. [CrossRef], [Google Scholar], [Publisher]

[26] A. Hung, J. Muscat, I. Yarovsky, S.P. Russo, *Surf. Sci*., **2002**, *513*, 511-524. [CrossRef], [Google Scholar], [Publisher]

[27] J. Cai, M. Philpott, *Comp. Mat. Sci*., **2004**, *30*, 358–363. [CrossRef], [Google Scholar], [Publisher]

[28] G. Oertzen, SL. Harmer, W. Skinne, Molimult, **2006**, *32*, 1207–1212**.** [CrossRef], [Google Scholar], [Publisher]

[29] K.S. Ahmed, K. Liu, Y. Fan, K. Louis Kra, J. Liu, M. Ntibahanana, M.Z. Salim, J.J. Pidho, M.E. Kouame, H.A. Moussa, H. Abba Ahmed, *ACS Omega*, **2022**, *48*, 43411–43420. [CrossRef], [Google Scholar] or [Publisher]

[30] A.R. Kiasat, J. Davarpanah, *J. Mol. Catal. A. Chem.,* **2013**, *373*, 46–54. [CrossRef], [Google Scholar], [Publisher]

[31] G.E. Davydyuk, Q.Y. Khyzhun, H. Kamarudin, G.L. Myronchuk, S.P.K. Danylchu, A.O. Fedorchuk, L.V. Piskach, M.Y. Mozolyuk, O.V. Parasyuk, *Phys. Chem. Chem. Phys*., **2013**, *15*, 6965–6972. [CrossRef], [Google Scholar], [Publisher]

[32] A.H. Reshak, *Phys. Chem. Chem. Phys*., **2014**, *16*, 10558–10565. [CrossRef], [Google Scholar], [Publisher]
[33] A.H. Reshak, *RSC Adv*., **2014**, *4*, 39565–39571. [CrossRef], [Google Scholar], [Publisher]
[34] J.P. Perdew, K. Burke, Y. Wang, *Phys. Rev. B*, **1996**, *54*, 16533–16539. [CrossRef], [Google Scholar], [Publisher]
[35] N. Bagdassarov, N. Bagdassarov, *Fundamentals of rock physics*, Cambridge University Press, **2021**, pp. 122–150. [Google Scholar]
[36] W. Aszkowicz, J.A. Leiro, *J. Alloy. Compd*., **2005**, *401*, 289–295. [CrossRef], [Google Scholar], [Publisher]
[37] A. Klamt, G. Schüürmann, *J. Chem. Soc*., **1993**, *2*, 799–808. [CrossRef], [Google Scholar], [Publisher]
[38] H. Nourmohamadi, V. Aghazadeh, M.D. Esrafili, *Surf. Interface. Anal*., **2021**, *55*, 110–118. [CrossRef], [Google Scholar], [Publisher]
[39] H. Nourmohamadi, M.D. Esrafili, V. Aghazadeh, *Appl. Surf. Sci*., **2020**, *495*, 143529–143540. [CrossRef], [Google Scholar], [Publisher]
[40] A.P. Chandra, A.R. Gerson, *Surf. Sci. Rep*., **2010**, *65*, 293–315. [CrossRef], [Google Scholar], [Publisher]
[41] S. Thinius, M.M. Islam, T. Bredow, *Surf. Sci*., **2018**, *669*, 1–9. [CrossRef], [Google Scholar], [Publisher]
[42] H. Nourmohamadi, V. Aghazadeh, M.D Esrafili, *Mater. Sci. Eng: B*, **2021**, *271*, 115243–114257. [CrossRef], [Google Scholar], [Publisher]

HOW TO CITE THIS ARTICLE

Valeh Aghazadeh, Bahram Rezai, Hossein Nourmohamadi*****. A Thermodynamic Investigation of the Interaction of Ferric (Fe^{3+}) Ion with (100, 110) Pyrite and (001) Chalcopyrite Surfaces Using the Density Functional Theory Study. *Adv. J. Chem. A*, **2023**, 6(3), 301-310.

DOI: 10.22034/AJCA.2023.397689.1378
URL: https://www.ajchem-a.com/article_174358.html